Observation of Dynamic Emittance at CESR with CLEO

Katherine Korbiak

Departments of Chemistry and Physics,
Wayne State University, Detroit, Michigan, 48202

Abstract

Dynamic emittance has been theoretically predicted, but never experimentally observed. Using Monte Carlo simulations of $\mu^+\mu^-$ events, an extensive study has been done on the factors that determine the resolution for the position and angular spread of the luminous region. Using these predicted resolutions, the beta and the emittance of the luminous region are extracted. Once emittance as a function of beam current has been calculated, it is observed that emittance does have a dependence on the beam current.

Introduction

Dynamic Beta was first observed at CESR with CLEO [1]. In that work, hadronic events are studied and it has been found that the resolution plots are not Gaussian distributions. Also, that technique does not allow for an easy measurement of the angular spread of particles from the luminous region. Therefore, only the theoretical values for emittance are used.

We have developed a new technique, using only the two-track $e^+e^- \rightarrow \mu^+\mu^-$ events. This technique allows for both a more accurate measurement of the beam position and for the direct measurement of the angular spread of the particles. An extensive study has been done on the position and angular distribution resolutions using Monte Carlo simulations, resulting in a much better understanding of what factors determine each resolution. The underlying widths of the collision region and the corresponding angular spreads in each dimension are then unfolded before beta and emittance are calculated as functions of beam current.

Background

The collision region is described by six parameters:

β_x Horizontal Beta

β_y Vertical Beta

ϵ_x Horizontal Emittance

ϵ_y Vertical Emittance

σ_z Bunch Length

σ'_z Beam Energy Spread

and given by the following equations:

$$\sigma_x = \sqrt{\beta_x \epsilon_x} \tag{1}$$

$$\sigma_y = \sqrt{\beta_y \epsilon_y} \tag{2}$$

$$\sigma'_x = \sqrt{\epsilon_x / \beta_x} \tag{3}$$

$$\sigma'_y = \sqrt{\epsilon_y / \beta_y} \tag{4}$$

$$\sigma_z = \sigma_{\text{bunch length}} \tag{5}$$

$$\sigma'_z = \sigma_E / E_{\text{beam}} \tag{6}$$

where

σ_x Horizontal Beam Width

σ_y Vertical Beam Width

σ'_x Horizontal Angular Spread

σ'_y Vertical Angular Spread

Finally, because the dimensions of the luminous region are being measured, rather than those of each beam, a factor of $\sqrt{2}$ must be considered due to the overlap of two Gaussian single-beam distributions.

Methods

The appropriate events for this analysis are the two-track $e^+e^- \rightarrow \mu^+\mu^-$ events. To measure the position of the beam spot, a box method, shown in Figure 1, has been used. The location of the beam spot's center is estimated based on previous measurements. The theoretical box is then centered around this point. The intercepts of tracks passing through the box are measured and the dimensions of the box are recalculated. As more tracks pass through the box, the calculation of the collision region becomes more precise. Thus the box becomes centered around the collision region and the error on its dimensions shrinks until the box is approximately the size of the beam spot.

Cuts are then made to include only the tracks with appropriate direction cosines. The error associated with measuring the momentum of each track is in the direction of motion of the track. Figure 2 shows that a track in the x,y plane with a small direction cosine in x will have a small error in the x direction, but a large error in the y direction. Thus this track only gives useful information in the x direction. Likewise, a track with a small direction cosine in y will give information only in the y direction because of the small associated error.

To measure the angular spread of the collision region, the angle between two tracks, θ, must be calculated. It is known that θ is much less than one radian, so it may be stated that

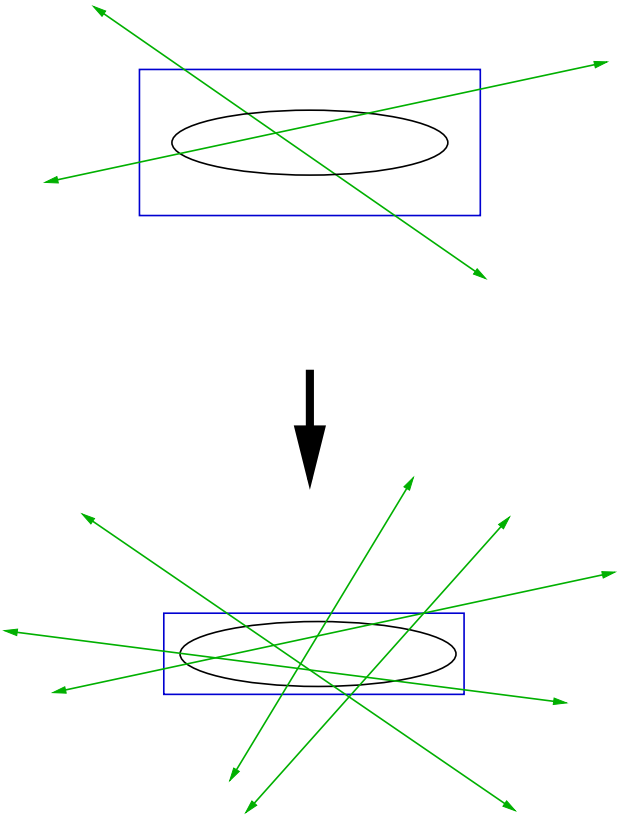

FIGURE 1. Measuring Position. Many tracks passing through the box allow for a very precise measurement of the beam spot.

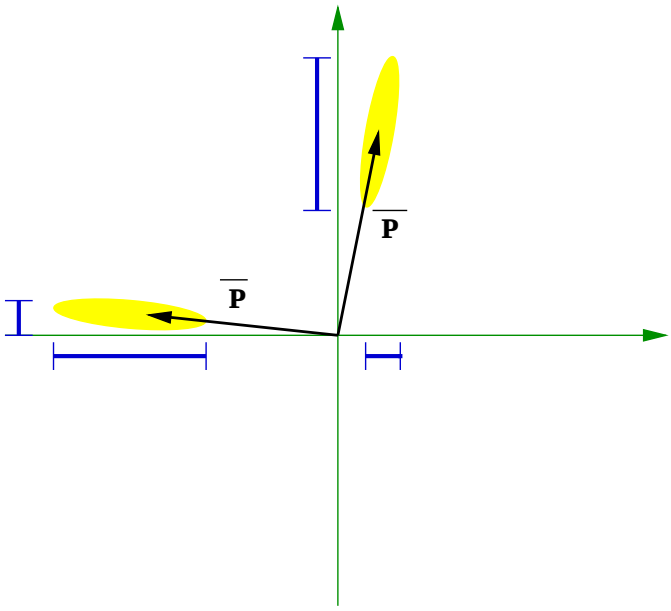

FIGURE 2. Determining Appropriate Slopes. The yellow regions represent the errors associated with the momenta of each track.

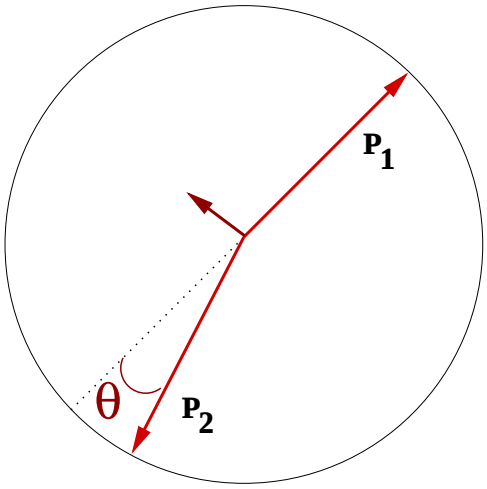

FIGURE 3. Measuring Collision Angle. The equation, Arc Length $= R\sin\theta$, is used with the approximations, $\sin\theta = \theta$ and Arc Length $\approx \sum p$, to measure θ.

$\sin\theta \approx \theta$. Figure 3 shows the sum of the momenta of the two tracks as an approximation for an arc length. Using the arc length equation, Arc Length $= R\sin\theta$, θ can be calculated with reasonable accuracy.

Now that we have a way to make measurements of the position and angular spread, the actual values for σ_x, σ_y, σ_z σ'_x, σ'_y and σ'_z can be extracted. To do this, the resolution associated with each of these variables must be completely understood. Then the underlying widths of each σ and σ' are extracted using the equation:

$$\sigma_{\text{measured}} = \sqrt{\sigma^2_{\text{real}} + \text{resolution}^2} \tag{7}$$

Finally, σ_x, σ_y, σ_z σ'_x, σ'_y and σ'_z are obtained as functions of beam current. From these values, the beta and emittance are plotted as functions of beam current so that any dynamic effects can be observed.

Understanding Resolution

An extensive Monte Carlo simulation of the appropriate events was performed to find the resolutions. The result is a better understanding of the resolutions and their dependencies. To determine the legitimacy of these results, the Monte Carlo expectation for the resolution in the y direction is compared to the width in the y direction. The underlying width of the beam in the y direction is on the order of 10μm. Because the underlying width in the y direction is less than its associated resolution, only this resolution is measured. The Monte Carlo generates a resolution of approximately 30μm, while the data has a 40μm resolution. Since these values are in good agreement, the Monte Carlo numbers are used to obtain the resolutions.

It has been determined that position resolutions depend on the number of rϕ hits and the number of z hits in the SVX. This dependence results from the dominance of the number of SVX hits on each track on the position resolutions. Figure 4 represents the resolution obtained before the data is binned by SVX hits, while Figure 5 shows a resolution after the data was binned by SVX hits. The best resolution was found for single tracks with three rϕ

and two z hits, so these types of tracks were used to measure the position of the collision region. Table 1 lists the Monte Carlo resolutions corresponding to each set of SVX hits examined.

TABLE 1. Monte Carlo Generated Position Resolutions

(rϕ,z) hits	x (μm)	y (μm)	z (μm)
(2,3)	30.3 $\pm$ 4.3	36.3 $\pm$ 3.9	61.3 $\pm$ 8.7
(3,2)	26.2 $\pm$ 1.2	35.5 $\pm$ 1.4	58.4 $\pm$ 2.7
(3,3)	30.9 $\pm$ 1.8	42.7 $\pm$ 2.2	61.0 $\pm$ 3.5

The resolutions for the angular distribution have slightly different dependencies. A dependence was found not only on the number of SVX hits, but also on the number of hits outside the SVX. Because both tracks are used to obtain the sum of momenta when looking for the collision angle, both tracks had to be taken into account. It has been found that the angular resolution has a dependence on the sum of rϕ hits and the sum of z SVX hits. Events that result in tracks with five or six rϕ and four, five, or six z hits are used for the best resolution. The momentum resolution is found to not only depend on the number of of SVX hits, but also on the number of hits outside the SVX. As the number of outer tracking hits, NHIT's, varies, the angular resolution varies according to the function:

$$\text{Resolution} = \text{C}\left(\frac{\text{A}}{\text{NHIT}} + \text{B}\right) \tag{8}$$

Values for A, B, and C were determined using Monte Carlo for each combination of SVX hits. Figure 6 represents the angular resolution in X as a function of NHIT's for tracks with six rϕ and five z hits. This dual dependence must be taken into account when measuring $\sigma'_x,\ \sigma'_y$ and σ'_z.

Results

Once the underlying widths for $\sigma_x,\ \sigma_y,\ \sigma_z\ \sigma'_x,\ \sigma'_y$ and σ'_z are obtained, their dependence on the beam current is extracted. It is observed that σ_x does decrease as the beam current increases, as shown in Figure 7. As expected, Figure 8 shows no variation of σ_y with the beam current. This is because σ_y represents the resolution, which does not have a dependence on the beam current. Both σ'_x and σ'_y show a dependence on the beam current as represented by Figures 9 and 10. They are both proportional to beam current. These values were then used to extract beta and emittance as functions of beam current. Figure 11 shows the dependence of the horizontal beta on the beam current. This beta clearly decreases as the beam current increases. The vertical beta, shown in Figure 12, does not vary significantly because σ_y represents the resolution. Figures 12 and 13 represent emittance as a function of beam current. In both instances, the emittance is seen to increase with the beam current. Hence these two plots are the first direct measurements of dynamic emittance.

Conclusions

A direct measurement of dynamic emittance has finally been made. There is also a

greater understanding of the factors that determine the resolution of any given parameter. Unfortunately, there is more work to be done in the following months. There is an inconsistency between the Monte Carlo and real data results for sigma-y which may be due to the hourglass effect. The properties of σ_z and σ'_z should also be explored. Finally, these results should be compared with the results obtained from the study on x,z hadronic events and with theoretical predictions of dynamic emittance.

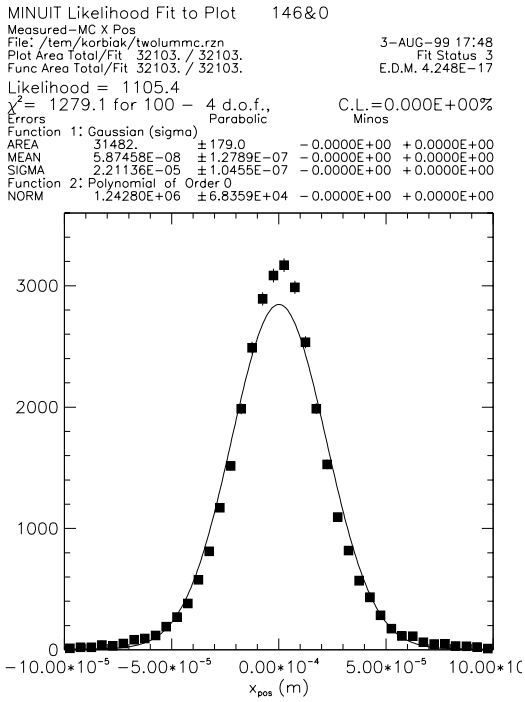

FIGURE 4. When the position resolution is plotted for all types of SVX hits, the fit is very poor

Acknowledgments

I am pleased to acknowledge Prof. D. Cinabro of Wayne State University for proposing this Research Experience for Undergraduates project, and for his undying support throughout the past months. Thank you for taking the time out of your busy schedule. I would also like to extend my gratitude to Prof. G. Bonvicini of Wayne State University and again to Prof. D. Cinabro for their dedication to this REU program and for their contributions in recruiting and preparing me for this program. Finally, I would like to thank Prof. D.G. Cassel of Cornell University for allowing our continued participation in this program and to everyone in the CLEO collaboration who helped make our stay in Ithaca, NY, very pleasant.

This work was supported by National Science Foundation REU grants PHY-9820306 and PHY-9731882 and research grant PHY-9809799.

Footnotes and References

1. D. Cinabro *et al.*, Phys. Rev. E **57**, 1193-1196 (1998) "Observation of the Dynamic Beta Effect at the Cornell Electron-Positron Storage Ring with the CLEO Detector", D. Cinabro, CBX 97-39, "Update on the Dynamic Beta Effect at CESR with CLEO", D. Cinabro, CBX 96-94, "Observation of Dynamic Beta Effects at CESR with CLEO".

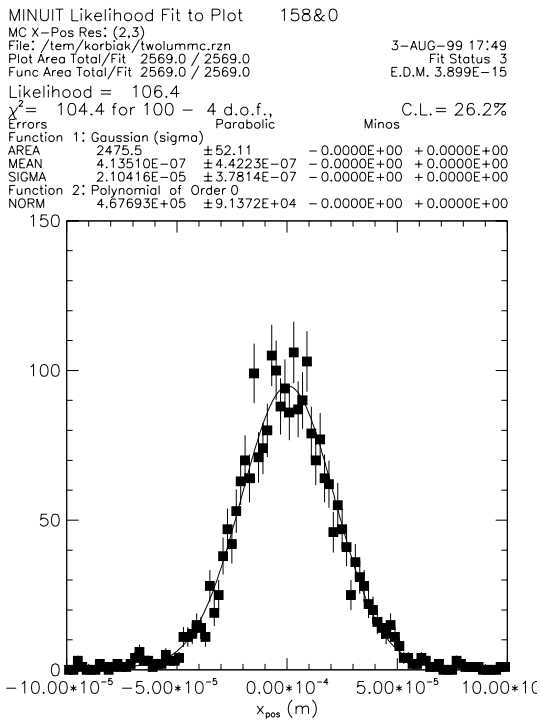

FIGURE 5. A good fit results when the resolutions are binned by SVX hits. This plot represents the resolution for the position in X for tracks with 2 rϕ hits and 3 Z hits

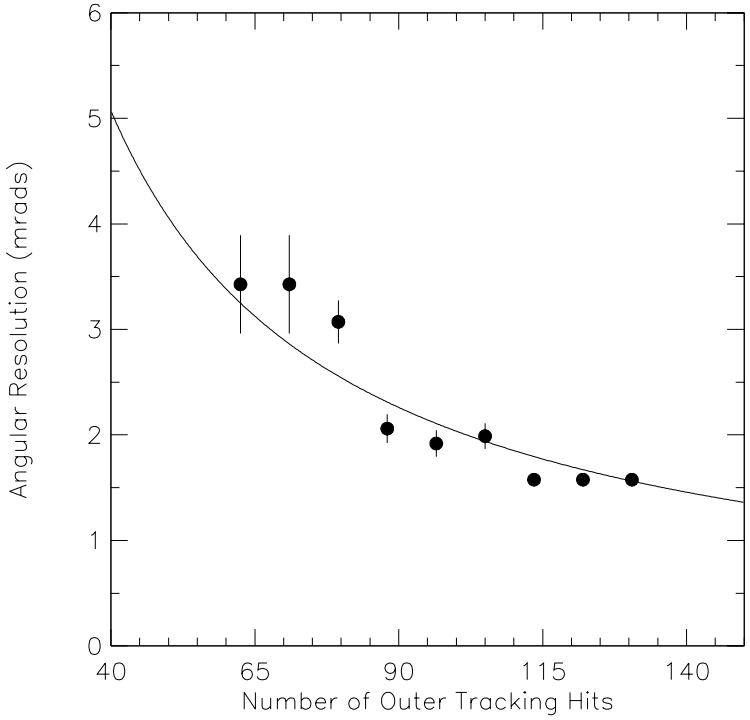

FIGURE 6. A representation of the parameterization of angular resolution for tracks with 6 rϕ and 5 z hits.

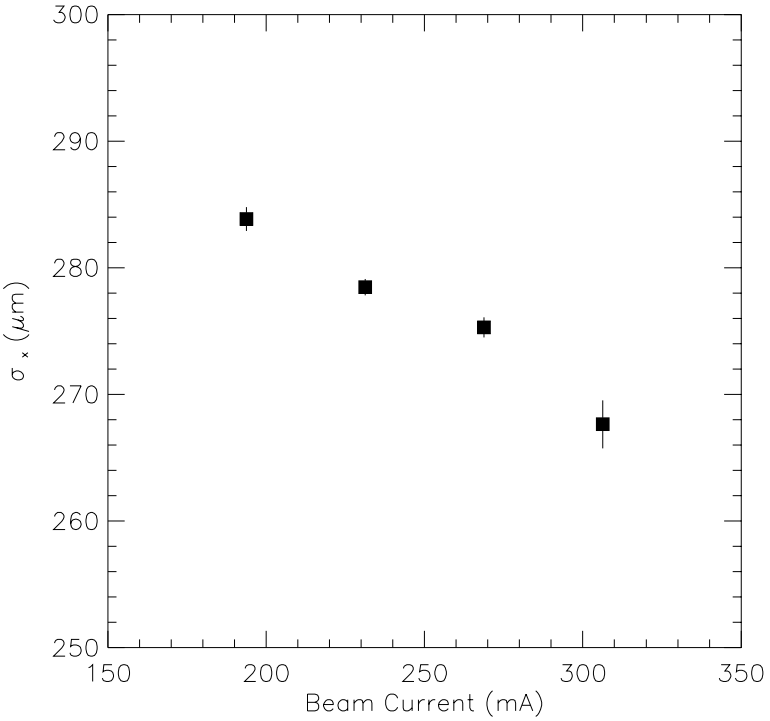

FIGURE 7. Plot of the width of the luminous region in x as a function of beam current.

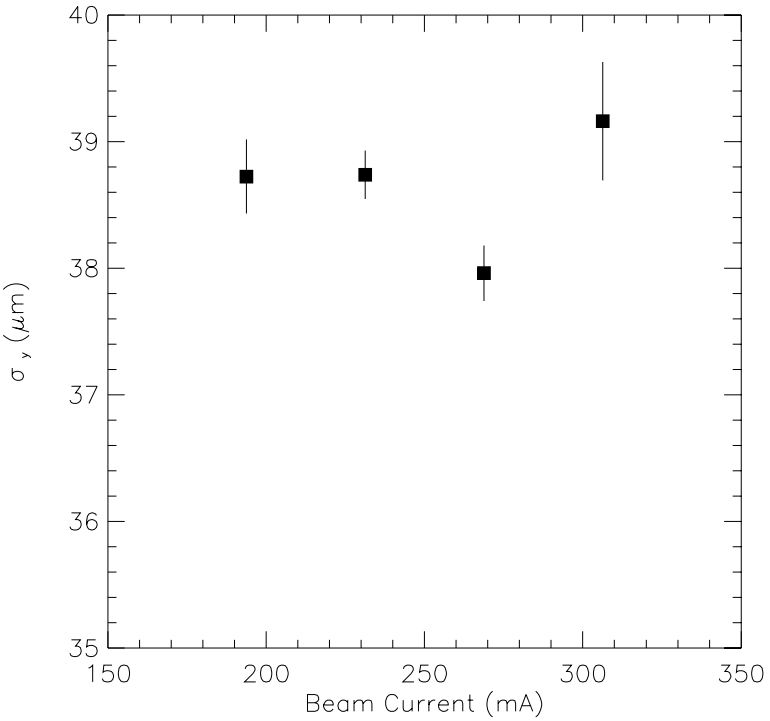

FIGURE 8. Plot of the width of the luminous region in y as a function of beam current.

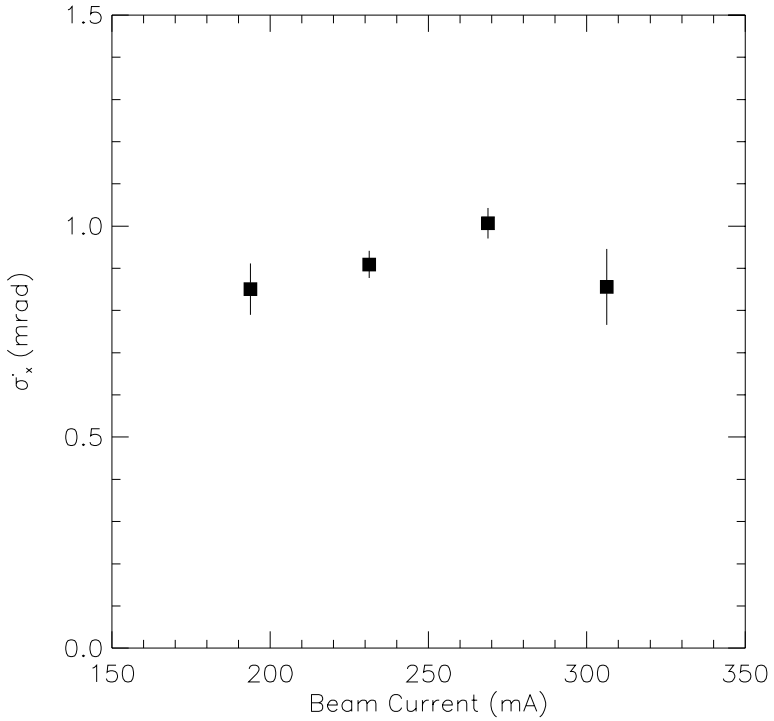

FIGURE 9. Plot of the angular spread of the luminous region in x versus the beam current.

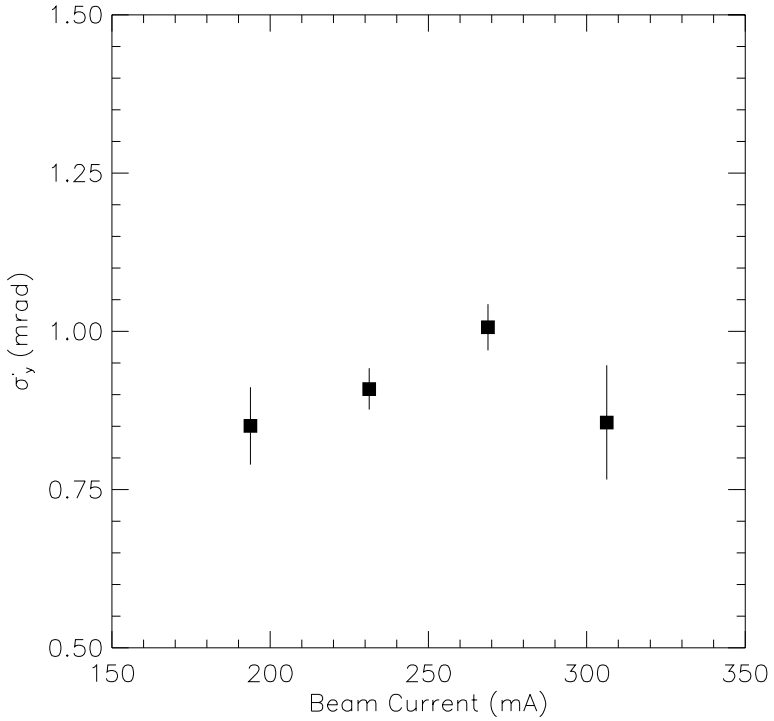

FIGURE 10. Plot of the angular spread of the luminous region in y as a functions of beam current.

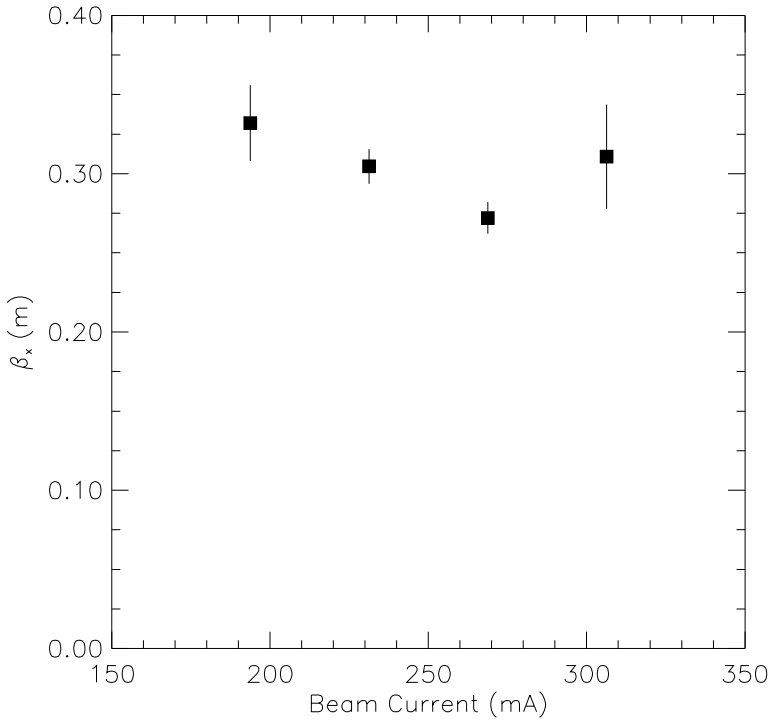

FIGURE 11. Horizontal beta as a function of beam current.

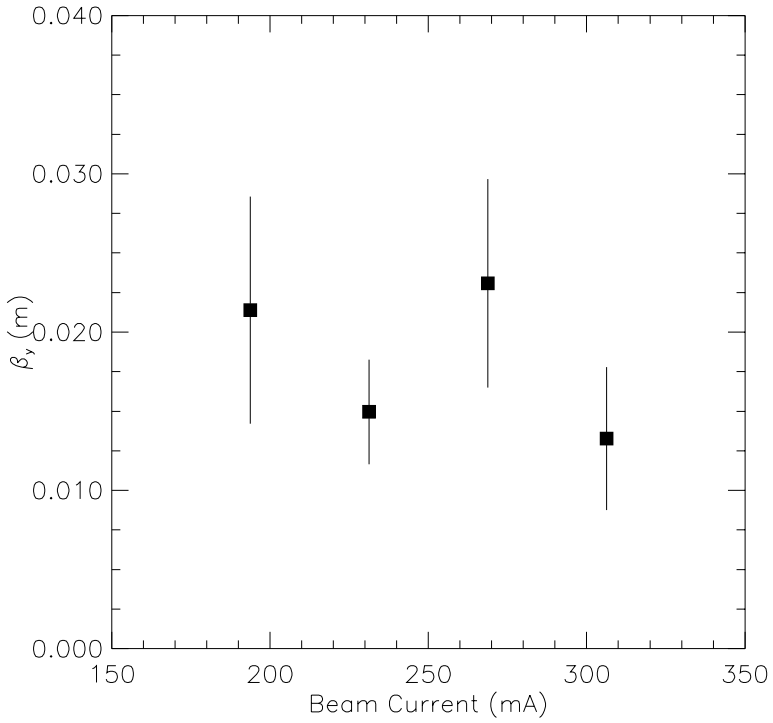

FIGURE 12. Vertical beta as a function of beam current.

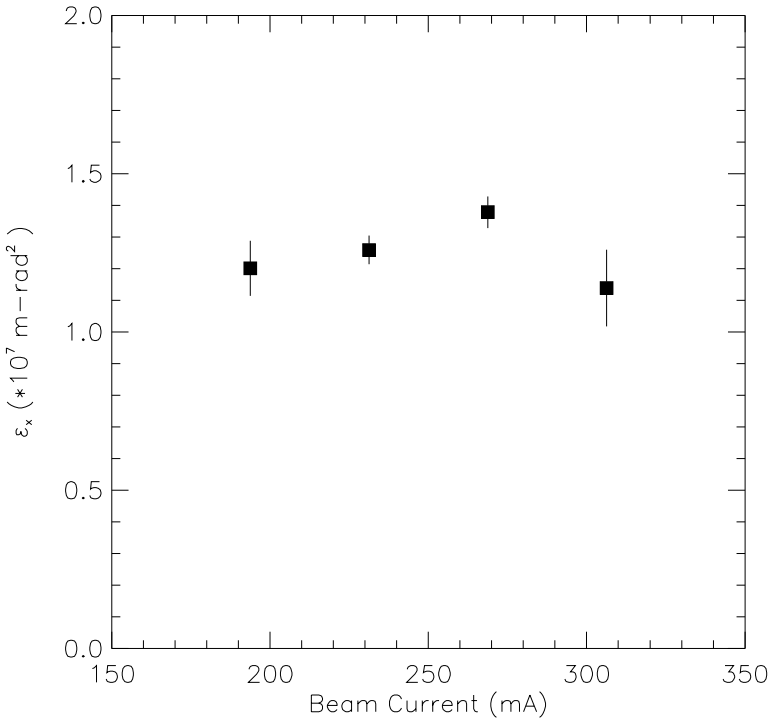

FIGURE 13. Horizontal emittance as a function of beam current.

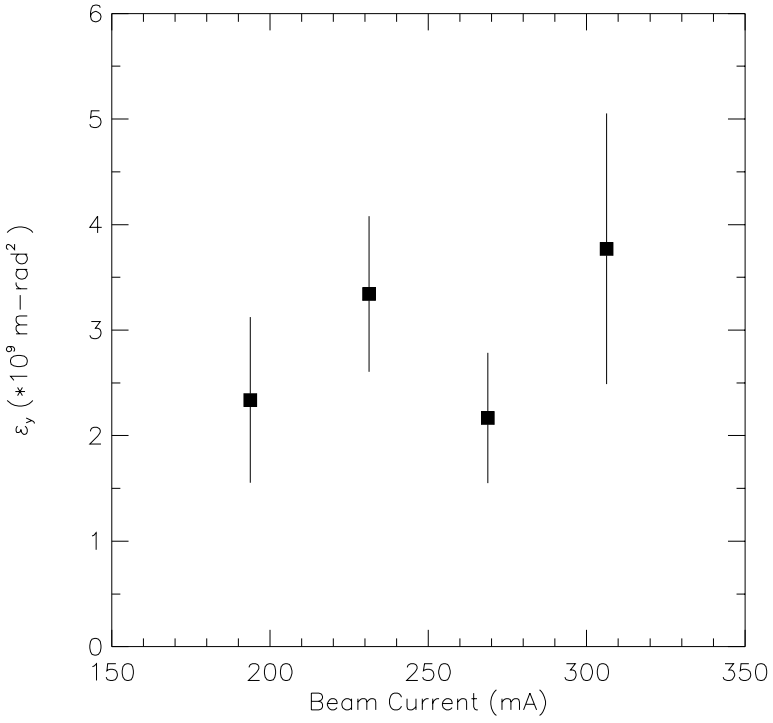

FIGURE 14. Vertical emittance as a function of beam current.